Pergamon

Journal of Structural Geology, Vol. 16, No. 2, pp. 263 to 276, 1994

0191-8141/94 $06.00+0.00

The external asymmetry of quartz *c*-axis fabrics: a linear approximation to its statistical description

C. FERNÁNDEZ-RODRÍGUEZ

Departamento de Geología y Minería, Universidad de Sevilla, 21819-Palos de la Frontera, Huelva, Spain

J. M. GONZÁLEZ-CASADO

Departamento de Geología, Universidad Autónoma de Madrid, 28049-Madrid, Spain

and

R. TEJERO

Departamento de Geodinámica, Universidad Complutense de Madrid, 28040-Madrid, Spain

(*Received* 14 *September* 1992; *accepted in revised form* 2 *April* 1993)

Abstract—When the skeletal outline of quartz *c*-axis fabrics is not clearly established, some testing procedures can be defined to attempt to verify the symmetry of the *c*-axis intensity distribution with respect to certain external reference axes (usually the principal axes of the finite strain ellipsoid). In this paper we propose a numerical method to describe that external asymmetry. Taking into account symmetry principles, a series of simplifications from the initial spherical distributions of axial poles to a final linear data distribution must be assumed. Two different parameters are derived: the external asymmetry factor, *Am*, upon which a test of external symmetry is established, and the statistical obliquity angle, α_f. The coupled use of both (*Am* and α_f) on non-isotropic fabrics is thought to be a reliable new kinematic criterion. This is shown by the analysis of a number of experimental, natural and theoretical quartz *c*-axis fabrics taken from the literature, where dextral shear senses imply almost invariably positive α_f angles for asymmetric fabrics. The method proposed here may also allow a quick numerical comparison of fabrics from different regions or sources.

NOMENCLATURE

Am	factor of external asymmetry of a quartz *c*-axis fabric
Am_c	critical value of Am for the test of asymmetry
C	statistic of *strength* of a fabric (Woodcock & Naylor 1983)
D	parameter of *amount of deformation* (Ramsay & Huber 1983)
I	statistic of *intensity* of a fabric (Lisle 1985)
K	*shape* of the ellipsoid representing an orientation tensor (Woodcock & Naylor 1983)
n	sample size
S	distance from the graph origin of a given point (orientation tensor) in the Woodcock diagram
S_{Am}	standard deviation of Am
S_u	statistic of uniformity of a fabric (Mardia 1972)
S_i	($i = 1, 2, 3$) normalized eigenvalues of the orientation tensor of a fabric
$\mathbf{t}_{\alpha/2}$	value of the t distribution for a given level of significance α
$\mathbf{V}_i$	($i = 1, 2, 3$) eigenvectors of the orientation tensor of a fabric
XYZ	principal axes of the finite strain ellipsoid
α	level of significance
α_f	angle of statistical obliquity
γ	shear strain
δ	acute angle between a given quartz *c*-axis and the X-axis of finite strain
ψ	angle of external fabric asymmetry (Law 1987)

INTRODUCTION

SINCE the first published quartz *c*-axis fabric diagram by Schmidt (1925), a large and growing number of studies deal with the crystallographic preferred orientation (CPO) of quartz aggregates. Special emphasis was placed on this field after the theoretical models presented by Lister and co-workers (e.g. Lister *et al.* 1978, Lister & Paterson 1979, Lister & Hobbs 1980) and by Etchecopar (1977). Recently, theoretical work (e.g. Etchecopar & Vasseur 1987, Jessell 1988a,b, Wenk *et al.* 1989), experimental research (e.g. Tullis *et al.* 1973, Tullis 1977, Dell'Angelo & Tullis 1986, 1989, Ralser 1990, Ralser *et al.* 1991) and studies of naturally deformed rocks (see reviews in Price 1985 and Schmid & Casey 1986) have demonstrated the utility of quartz fabrics in the analysis of strain symmetry, in the determination of palaeostresses or active slip systems, and finally as a shear-sense criterion in ductile shear zones (for a review see Law 1990). A number of controversies arose in attempts to develop each of these topics. From a theoretical point of view, many of these controversies are a consequence of the so-called inverse problem of fabrics (Lister & Price 1978, Schmid & Casey 1986), that is, the fact that knowledge of the final result—the fabric—does not allow complete determination of all the factors (including the intrinsic and the extrinsic factors of Hobbs 1985) that contributed to its development.

The use of CPOs as kinematic indicators in ductile shear zones has received considerable attention during the last two decades. With respect to the study of quartz *c*-axis fabrics, two different kinematic criteria have been proposed: the first is based on pole-figure topology, and rests on the symmetry of the skeletal outline or on the leading edge principle (Lister & Williams 1979, Lister &

Hobbs 1980, Behrmann & Platt 1982); the second pays attention to the asymmetrical intensity of the *c*-axis pole distribution (e.g. Laurent & Etchecopar 1976, Bouchez & Pécher 1976, 1981, Bouchez 1977). Some of the risks related to these methods have been pointed out by García Celma (1982), Bouchez *et al.* (1983), Passchier (1983), Simpson & Schmid (1983) and Law (1990).

When the skeletal outline definition is unequivocal, it is possible to measure a set of angular parameters that allow the *c*-axis fabric asymmetry to be quantified. Some of these angles can be measured with respect to axes belonging to an external framework; others are established in terms of internal axes of the fabric. They are the external and internal symmetry parameters, respectively (Behrmann & Platt 1982, Platt & Behrmann 1986). The notation and geometrical meaning of these parameters differ between authors (cf. Simpson 1980, Behrmann & Platt 1982, Law 1987, Mancktelow 1987).

The skeletal outline of a fabric is not always easy to obtain (Simpson & Schmid 1983). If this is the case it could be useful to define some independent parameter, based on the asymmetry of the distribution intensity. When such a parameter is statistically established, it is possible to control the errors concerning the symmetry estimation. This could also allow the comparison of fabrics with different origins.

In this paper we propose a number of statistical parameters that provide a numerical evaluation of the intensity of the external asymmetry via a decision test. The viability of the method has been checked using several natural, experimental and theoretical quartz *c*-axis fabrics derived from the recent literature.

THE METHOD

Theoretical considerations

Following Bunge (1985) the complete description of a fabric is not practical as it implies an exact knowledge of the compositional nature and crystal orientation for each point in the aggregate. Instead of that, it is more convenient to give a partial statistical characterization of the fabric. In accordance with the Curie symmetry principle, convincingly applied to geology by Paterson & Weiss (1961), the symmetry of a crystallographic fabric is a consequence and a key for the inference of the imposed deformation path symmetry, provided that the original crystallographic fabric can be considered as statistically isotropic and that the kinematic description of the deformation remains constant (Lister & Hobbs 1980). Deformation mechanisms have no influence upon the validity of this assumption (Wenk & Christie 1991), and therefore it is expected to be of great interest in structural geology. It constitutes the theoretical basis for the use of quartz *c*-axis pole figures as a kinematic criterion (Wenk & Christie 1991).

Strictly speaking a *c*-axis pole figure is only a sub-fabric of the whole crystallographic fabric. It is usually preferable to obtain more complete statistical descriptions, such as the orientation distribution function (ODF; Bunge 1969, Schmid *et al.* 1981) that consists of a mathematical combination of several sub-fabrics. However, when the technical and mathematical facilities required to establish an ODF are not readily available, the structural geologist must rely upon the analysis of single sub-fabrics.

Note that following the Curie principle the symmetry of a whole fabric can be equal or less, but never greater than that shown by the sub-fabric of a particular element (Turner & Weiss 1963). Therefore, symmetric quartz *c*-axis sub-fabrics can belong to an asymmetric whole fabric, and this was shown in several studies of natural quartz aggregates (e.g. Schmid & Casey 1986, Law 1987). Assuming an originally isotropic CPO, we should conclude that asymmetric quartz *c*-axis fabrics imply non-coaxial deformational histories, while symmetric *c*-axis fabrics do not imply necessarily coaxial deformation histories (e.g. Schmid & Casey 1986).

When attempting to analyse the sub-fabric of a crystallographic element as for example the *c*-axes in quartz, it is advisable to establish beforehand the pole or intrinsic symmetry of that element (Weiss & Wenk 1985). The pole symmetry depends on the point group of the crystalline structure. For instance, in quartz, whose point group is 32, the *c*-axes are located in coincidence with the three-fold rotation axes. Taking into account the enantiomorphic character of the quartz crystallographic lattice, the *c*-axes are defined as *axial chiral* directions (Weiss & Wenk 1985). The axial character explains the fact that only one hemisphere suffices to represent their distribution in a spherical projection. On the other hand, the right- or left-handed chiral character of single crystals is seldom determined in the study of quartz aggregates. That implies that the *c*-axis pole figures must be considered as a combination of data with two possible chiral senses.

Finally, when considering a polycrystalline aggregate the pole distribution is largely independent of the lattice symmetry. In the case of quartz, the *c*-axes are centrosymmetric elements, and then the symmetry of aggregates consists of only five different point groups (Paterson & Weiss 1961, Weiss & Wenk 1985): spherical or isotropic (∞/m ∞/m), axisymmetric (∞/m 2/m), orthorhombic (2/m 2/m 2/m), monoclinic (2/m) and triclinic ($\bar{1}$); where '∞' and '2' are proper rotation, 'm' mirror planes and '$\bar{1}$' a center of symmetry. Considering a situation of statistical homogeneity, the five point groups could be transformed in space groups by means of arbitrary translations in all the spatial directions (Paterson & Weiss 1961). From a geological point of view, the isotropic point group corresponds to sub-fabrics without crystallographic preferred orientation. The axisymmetric and orthorhombic point groups could be ascribed to the broader and more diffuse class of symmetric sub-fabrics; and the monoclinic and triclinic groups would be associated with asymmetric sub-fabrics.

In short, the quartz *c*-axis sub-fabrics are partial statistical descriptions, easy to obtain by optical

methods and to represent in conventional hemispherical projections, and are promising as a kinematic criterion when symmetry principles are considered. In the following sub-sections we will review the statistical procedures to evaluate the isotropy of a pole figure, and then we will propose a method to determine the degree of asymmetry for a non-isotropic sub-fabric.

Isotropy and strength

Fabrics derived from undeformed rocks in nature are not truly isotropic, but they are statistically isotropic. During deformation processes a significant deviation from that isotropy is usually achieved. In order to define the isotropic character of fabrics several procedures have been developed. The more suitable of them are based on the computation of the eigenvalues of the orientation tensor divided by the sample size (normalized): S_i, i = 1,2,3 (Scheidegger 1965). The following tests attempt to elucidate the isotropy on that ground.

(1) A randomness non-parametric test suggested by Woodcock & Naylor (1983). The parameter C is estimated in terms of the maximum (S_1) and minimum (S_3) normalized eigenvalues of the orientation tensor:

$$C = \ln (S_1/S_3). \tag{1}$$

Critical values of C separate the isotropic from the non-isotropic fabrics.

(2) A parametric test based on the Bingham distribution, proposed by Lisle (1985). The parameter I, related to the uniformity statistic of Mardia (1972), S_u, defines the degree of isotropy:

$$I = (15/2) \sum_{i=1}^{3} (S_i - 1/3)^2 \qquad S_u = I \cdot n, \tag{2}$$

where n is the number of poles the sample and S_i the normalized eigenvalues of the orientation tensor. The fabric is considered to be statistically non-isotropic when I exceed a given critical value.

Once this decision procedure leads to recognition of fabric anisotropy, the degree of preferred orientation (the strength) can be adequately explained in terms of the C and I parameters. In addition both the strength and the shape of a given fabric can be graphically represented in a Woodcock diagram (Woodcock 1977, Woodcock & Naylor 1983). This can be considered as an equivalent to the Flinn diagram for deformation, but with the logarithmic eigenvalue ratios $\ln(S_1/S_2)$ and $\ln(S_2/S_3)$ as ordinate and abscissa, respectively. Similarly a K (shape) parameter is defined as $K = \ln(S_1/S_2)/\ln(S_2/S_3)$, with the $K = 1$ line as a diagonal running from the bottom left to the right top of the diagram. The origin of the graph represents a spherical or isotropic fabric. Girdle distributions have K values lying between zero and unity, and cluster distributions plot in the $K > 1$ field. A third strength parameter could be defined as the distance between the origin of the Woodcock graph and the point marking the position of a particular orientation tensor. The resulting value is:

$$S = \{[\ln (S_1/S_2)]^2 + [\ln (S_2/S_3)]^2\}^{1/2}. \tag{3}$$

This expression is formally identical to that of the parameter D, suggested by Ramsay & Huber (1983) as a measure of the 'amount of deformation' recorded by a strain ellipsoid. Nevertheless S and D express values taken by the eigenvalues or by the principal plane strain ratios, respectively; therefore they should not be considered as factors with an absolute significance (Ramsay & Huber 1983). No attempt to elaborate a decision test for isotropy based on S has been made in this work.

The procedures outlined above are not strictly valid when applied to multimodal samples or to distributions with low internal symmetry (Woodcock 1977). However, in our experience they provide an acceptable approximation to the randomness evaluation when dealing with those complex non-unimodal fabrics.

Asymmetry

Only when the anisotropic character of the c-axis sub-fabric is demonstrated should we pass to the following step in the method, i.e. to describe the fabric as pertaining to either a symmetric or an asymmetric point group. As stated in the Introduction the symmetry can be referred to some external axes or, independently from these, to internal symmetry operators as a measure of rotational invariance between different parts of the fabric. Some parametric tests have been proposed to evaluate this internal symmetry (e.g. Mardia 1972), but they are only relevant to axisymmetric distributions, and only once the sample was proved to correspond to a specific statistical distribution (generally the Bingham distribution). In orthorhombic and monoclinic fabrics the internal symmetry is characterized by several angular parameters easily obtained from the skeletal outline (Behrmann & Platt 1982, Law 1987).

The external symmetry is often defined with respect to the XYZ-axes of the finite strain ellipsoid. As shown by Simpson & De Paor (1993), the choice of foliation as a reference frame is not a problem when we only attempt to characterize the sense of rotation of the flow and not the numerical value of vorticity. In some cases the skeletal outline of the fabric can be unequivocally established and directly compared to that external frame. Otherwise we must look for additional criteria to ascertain the degree of external symmetry of the sample. An attempt to resolve this problem is presented in the following paragraphs.

In Fig. 1(a) a characteristic orthorhombic distribution is displayed (type I crossed-girdle pattern of Lister 1977, with internal symmetry: 2/m 2/m 2/m); this fabric is clearly symmetric, also with respect to the external XYZ-axes, because these axes coincide with the two-fold internal rotation axes (2_1, 2_2, 2_3), while the principal planes of the strain ellipsoid correspond to mirror planes (m_1, m_2, m_3). This is an internal and external ortho-

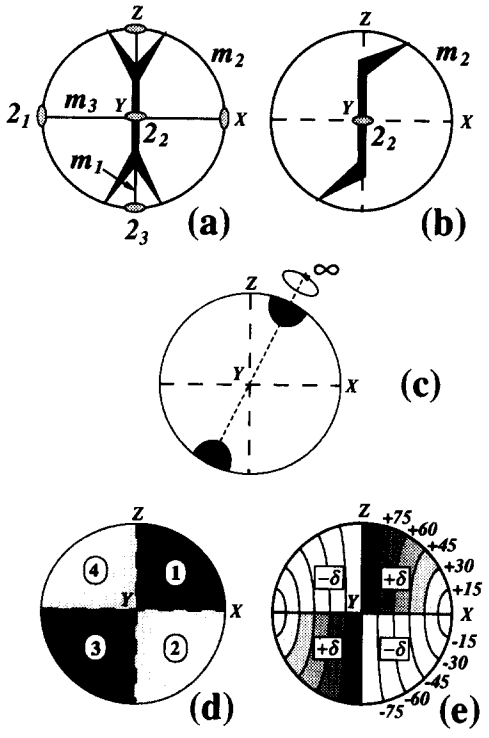

Fig. 1. External and internal symmetry elements in quartz *c*-axis crystallographic fabrics. (a) Type I crossed-girdle with orthorhombic external symmetry. (b) Single kinked girdle, monoclinic with respect to the *XYZ* frame. (c) Single maximum with axisymmetric internal symmetry and monoclinic external symmetry with respect to the *XYZ* axes. Only the ∞-fold rotation axis is shown . (d) Quadrant division of the projection hemisphere. (e) definition of the value and sign of angle δ, with isolines every 15°. Thin discontinuous line: ∞-fold rotation axis; ellipses: two-fold rotation axes (2_1, 2_2, 2_3); heavy lines: mirror planes (m_1, m_2, m_3); *XYZ*: principal axes of the finite strain ellipsoid.

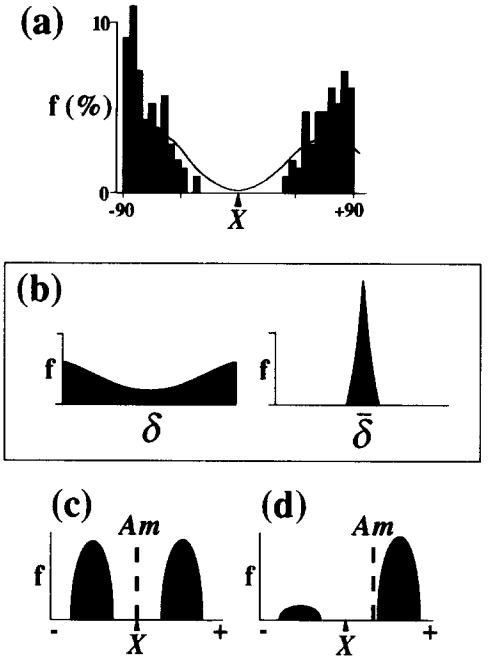

Fig. 2. Frequency linear histograms of δ. (a) Sample 14W-10-16 of Compton (1980). Interval of classes, 5°. A smoothing curve is also shown. (b) Normal distribution of means selected at random (right) from a non-normal population of δ values (left), when the extension of the sample is large (n = 25); from Lapin in Davis (1986). (c) & (d) Position of *Am* with respect to *X* for a symmetric (c), and an asymmetric fabric (d). See text for explanation.

rhombic fabric, that is, a symmetric fabric. Figure 1(b) shows a monoclinic fabric (single kinked girdle, with internal symmetry: 2/m), asymmetric with respect to the *XYZ*-axes. Here only the *Y*-axis coincides with a binary axis (2_2); and the same situation holds with the planar elements, the $|XZ|$ plane corresponding to m_2. It is an internal and external monoclinic fabric, that is, an asymmetric fabric. Both models represent a large number of natural, experimental and modelled quartz *c*-axis fabrics. In fact a direct correlation between internal and external symmetries in quartz *c*-axis fabrics can be inferred from data published to date (see e.g. Price 1985, Schmid & Casey 1986). Note, however that external asymmetry and internal symmetry is also possible, as when we find a single point maximum or a straight single girdle oblique to the external axes (Fig. 1c). In these cases the proper rotation axes (∞, 2) and mirror planes (m) deviate from the *XYZ* finite strain axes and, as a consequence, internal axisymmetric distributions degenerate to monoclinic or perhaps triclinic external symmetries. The general condition for external symmetry is the full coincidence of the external axes and the operators of internal symmetry. To discriminate between external symmetry and asymmetry it is therefore merely necessary to check the statistical recurrence of a particular distribution of axial elements in a fabric when a rotation of 180° around the axes 2_1 and 2_3 (*X* and *Z*), or a reflection through the mirror planes m_1 and m_3 ($|YZ|$ and $|XZ|$), has been performed. Similar checking rotations could be proposed for axisymmetric fabrics (Fig. 1c).

When fabrics exhibit axisymmetric, orthorhombic or monoclinic distributions an accurate simulation of the rotations and reflections required to prove their external symmetry can be provided by first a division of the projection hemisphere into four quadrants according to the principal planes of the strain ellipsoid (Fig. 1d) and second a comparison between the two quadrant pairs: first and third vs second and fourth. The equivalence condition between them can be expressed as a statistical comparison of pole distribution intensity, established not only on the number of poles, but also on their position inside each quadrant. Unfortunately, as far as we are aware, no testing procedure has been fully developed to account for this specific operation, although related topics are discussed in systematic treatises of statistical theory and methodology for spherical data (for a review see Fisher *et al.* 1987). A way to establish a simple numerical approximation to this comparison could be made by the following approach.

(1) The two angular co-ordinates describing the position of a pole with respect to the *XYZ* framework are transformed in a single angular value: δ. This is the acute angle between each *c*-axis and the *X*-axis of the strain ellipsoid. δ takes a positive value when the pole is located inside the first and third quadrants, and a negative value otherwise (Fig. 1e). A typical distribution of δ values from a quartz *c*-axis fabric is shown in Fig. 2(a). This step converts spherical axial data into circular axial

data. The transition from the three Euler angles necessary to describe the orientation of one crystal in a complete fabric description to the two angles of a single sub-fabric and then to the circular distribution of δ values seems to represent ordered steps of a progressive simplifying procedure, and the Curie principle will govern the interpretations concerning symmetry in all stages. In the process only one dimension remains and the information concerning the exact position of each point or cluster of points within a given quadrant is reduced to a mere two-dimensional gradient from the X-axis to the $|YZ|$ plane (Fig. 1e). As a result any information about the skeletal outline disappears, and only rough differences in distribution intensities between quadrants can be analysed (Fig. 2a). For instance, a c-axis located near to Y will give the same δ value than a c-axis close to Z (Fig. 1e). A geometrical image for the significance of this process can be gained if the fabrics from Figs. 1(a)–(c) are superposed onto the net in Fig. 1(e). Fabrics with external asymmetry (Figs. 1b & c) must have more points within one of the quadrant pairs and therefore they will develop a statistical preference for positive or negative δ values. In Bouchez (1977), Etchecopar (1977) and Lister & Hobbs (1980) similar, but not identical, single angular values are obtained, and they are represented in a fashion that closely resembles our Fig. 2(a).

(2) If the position of the X-axis (the zero direction) is perfectly established in the sample, the δ values can be treated as corresponding to a linear distribution. The linear histogram in Fig. 2(a) is a graphical representation of this conversion. Additional information concerning the distribution of poles will not be lost during this stage. Provided that a sufficient number of poles are available (we will consider this aspect later), the central limit theorem makes it possible to use testing procedures based on the normal distribution to check different properties of the fabric (Fig. 2b). The linear distribution of δs in a sample can be described by various statistics, as for instance the arithmetic mean (Am) or the standard deviation (S_{Am}). Here Am is considered as an authentic asymmetry factor, in fact Am is believed to lie close to O (the X axis position) when the fabric is symmetric (Fig. 2c). In contrast, clearly asymmetric fabrics will have Am values statistically different from O, as deduced from its tendency towards positive or negative δ values (Fig. 2d). A decision rule must be designed in order to constrain the significance of that deviation. The hypothesis—often referred to as a null hypothesis—that must be tested during the decision procedure is that the mean of the parent population from which the sample was obtained is equal to O; it is a testing against symmetry. Following standard procedures (Davis 1986) critical values of Am for the test are given by:

$$Am_c = \pm \mathbf{t}_{\alpha/2} \cdot S_{Am} \cdot n^{-0.5}, \qquad (4)$$

where $\mathbf{t}_{\alpha/2}$ is the value of the $\mathbf{t}$ distribution for a given level of significance (α); S_{Am} is the standard deviation of the sample, and n is the number of measured poles. Equation (4) separates an acceptance region bounded by the critical Am_c values from a rejection field, outside these critical values. When the Am for a particular sample fall within the rejection field the sub-fabric is said to show external asymmetry. If the position of X is unknown or dubious the simplification cannot be made, due to the lack of invariance shown by circular distributions when the origin is variable: when angular data (δ) are treated in a linear form the value taken by some relevant descriptive measures like the arithmetic mean will strongly depend on the position of the zero direction (e.g. Mardia 1972).

Loss of information about the location of c-axis maxima or girdles can preclude the use of this method on very irregular triclinic fabrics, in particular when maxima alternate so that the final result is external symmetry. For an explanation the Curie principle may be again adduced: asymmetric distributions of δ values imply asymmetric quartz c-axis sub-fabrics, but symmetric distributions of δs do not necessarily imply symmetric sub-fabrics. In a sense almost every natural quartz c-axis fabric can be considered as a triclinic fabric; fortunately they are far from the irregularity already mentioned and often keep a structural resemblance to monoclinic or orthorhombic distributions (see examples in Price 1985).

Statistical obliquity

As we have seen above and in pole figures with a well-defined skeletal outline, it is common to use angular parameters as kinematic criteria. The external asymmetry is often described by the so-called *obliquity* angle, whose meaning is not clearly established and can be quite variable for different authors (e.g. Brunel 1980, Simpson 1980, Law 1987, 1990, Mancktelow 1987). Once again, when the fabric skeleton is not well marked it could be preferable to establish a factor based on more objective grounds. Let $\mathbf{V}_1$, $\mathbf{V}_2$ and $\mathbf{V}_3$ be the eigenvectors related to the three eigenvalues of the orientation tensor: S_1, S_2 and S_3, respectively. Planes connecting the eigenvectors are here considered as the *statistical skeleton* of the fabric. Depending on the K value of the sample, a *statistical obliquity angle* (α_f) can be defined as in Fig. 3. For $K < 1$, i.e. when S_1 and S_2 are both large and S_3 small so that the orientation of plane $|\mathbf{V}_1\mathbf{V}_2|$ is fixed, α_f is the angle measured in the $|XZ|$ plane between the Z axis and the intersection of the planes $|XZ|$ and $|\mathbf{V}_1\mathbf{V}_2|$ (Fig. 3, left). For $K > 1$, S_2 and S_3 are both small and the orientation of $|\mathbf{V}_1\mathbf{V}_2|$ can be quite variable depending on slight fluctuations in the c-axis distribution. However, $\mathbf{V}_1$ is fixed and consequently α_f is established as the angle between the planes $|YZ|$ and $|\mathbf{V}_1\mathbf{Y}|$ (Fig. 3, right). As usual XYZ are external reference directions corresponding with the principal finite strain axes. A sign criterion for α_f is also shown in Fig. 3. In our experience only isotropic or very irregular triclinic distributions display anomalous orientation of the eigenvectors, reducing the reliability of α_f. The difference between Am and α_f is clearcut: Am is a statistic based on a comparison in the distribution intensity

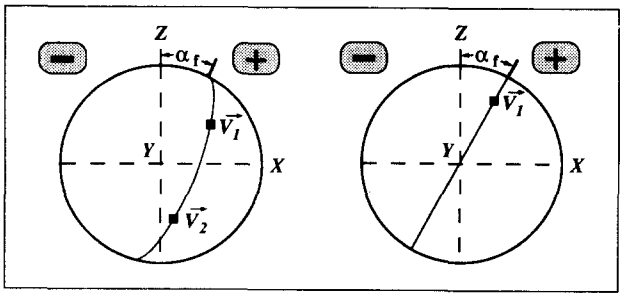

Fig. 3. Statistical obliquity angle α_f based on the computation of the orientation tensor eigenvectors. Definition and sign of α_f for fabrics with $K < 1$ (left) and $K > 1$ (right). $\mathbf{V}_1$ and $\mathbf{V}_2$ are the eigenvectors related to the maximum and intermediate eigenvalues, respectively.

between parts of the fabric, and acts as a diagnostic tool for asymmetry; α_f is more a geometric factor indicating the tilting of the statistical skeleton with respect to the XYZ frame.

The method just described allows us to describe the symmetric or asymmetric character of a quartz c-axis fabric. When the external asymmetry has been demonstrated in a non-isotropic fabric, the statistical obliquity angle may be used as a kinematic criterion once one has assumed a physical model of fabric development that indicates the sense of tilting that must result from a specific shear sense in non-coaxial flow. In order to test the viability of this procedure some examples of quartz c-axis fabrics from the literature will be analysed. They have the following characteristics.

(a) They result from theoretical simulations, from experiments or from naturally deformed rocks.

(b) In almost every sample the deformation history, the finite strain value, the developing conditions and the initial fabric are well established.

(c) All the fabrics have been published in spherical projection and as pole representations, without isodensity contours. The fabrics were digitized, transformed to numerical computer files, and analysed through the procedures outlined above.

(d) The figures corresponding to non-coaxial deformations were all standardized and digitized to represent a dextral shear sense.

ASYMMETRY ANALYSIS OF NATURAL, THEORETICAL AND EXPERIMENTAL FABRICS

Table 1 summarizes the sources of analysed fabrics and the statistical results. The fabrics have different deformation histories, either coaxial or non-coaxial. In an attempt to compare the deformation intensity with the degree of fabric isotropy, and with the asymmetry of pole distributions, the following parameters have been computed: D,I,C,S, Am and α_f. A complete description of each sample is given in the works mentioned in Table 1.

The decision concerning the isotropy character was taken following both the Lisle (1985) and the Woodcock & Naylor (1983) tests. The results were invariably coincident, and are expressed in Table 1. Minimum values of D,I,C and S belong to samples defined as isotropic.

The results of the external asymmetry tests are also plotted in Table 1. The decision involves a level of significance of 0.01. Asymmetric fabrics clearly prevail for non-coaxial deformation paths. For these latter histories a striking coincidence between the increase in the strain intensity factor (D), the fabric strength parameters (I,C,S), and the external asymmetry (Am) was found. These topics will be considered at length later in this section. The angle α_f separates fabrics with a dextral obliquity (positive) from those with a sinistral one (negative). The largest obliquity values are also associated with the fabrics resulting from non-coaxial deformation histories.

A better understanding of results in Table 1 can be gained if the principal relations among the statistical parameters are expressed in a graphical form. A brief account of these graphs is added in the following subsections.

Orientation tensor: shape evolutions and fabric strength

The c-axis fabrics are plotted in logarithmic Woodcock diagrams (Fig. 4). Fabrics derived from coaxial models based on the Taylor–Bishop–Hill (TBH) theory follow three different paths, according to their deformational evolution: axisymmetric flattening, plane strain or axisymmetric extension (Fig. 4a). This statistical characterization shows the simplicity of single clusters ($K \approx \infty$) formed during axial flattening, or that of perfect single girdles ($K \approx 0$) normal to X in axial extension (Price 1985). The intermediate nature of the crossed girdles in plane strain is a somewhat more surprising result, the explanation of which is believed to lie in the essentially double-maximum or incomplete girdle distribution of c-axes along the $|YZ|$ plane. These paths differ from those of non-coaxial deformation models that show convex upwards trajectories (Fig. 4b). The evolution from broad clusters ($K > 1$) in the first stages of shear strain, to crossed girdles ($K = 1$) and finally to sharp single girdles ($K < 1$) in the last episodes is the main inference to be extracted from the convex paths.

In the fabrics derived from theoretical models there is a close relationship between the strain intensity factor (D) and the strength parameters (I,C,S) (Table 1), as was already noticed in the past (e.g. Lister *et al.* 1978, Dell'Angelo & Tullis 1986). Isotropy is rejected for D values between 0.14 and 0.4 (Table 1). This implies a critical shortening of about 23% in axisymmetric flattening, and shear strain values of around 0.57 for simple shear deformations. These results are slightly lower than values mentioned in the literature (e.g. Etchecopar 1977, Lister & Hobbs 1980, Hobbs 1985, Jessell 1988b). A reduction in the strength of fabrics for high D values as predicted for instance by Lister & Hobbs (1980) or Hobbs (1985) is not obvious in some of our results for non-coaxial models, where a strong increase in I,C or S with D is particularly obvious (Table 1). However, this should not be considered as a hint against the suggestion

Table 1. Summary of results for the digitized fabrics (A*m* in absolute value). See text for details

Strain history	Fabric	Source	Number*	*D*	*I*	*C*	*S*	Isotropy	|A*m*|	Asymmetry ($\alpha = 0.01$)	Obliquity (αf)†
Coaxial models											
Initial fabric	LH.1	Lister & Hobbs (1980)‡	1	0.00	0.02	0.23	0.16	Yes	—	—	—
Axisymmetric flattening	LH.6	Model quartzite. B	2	0.77	0.27	0.78	0.56	No	3.69	No	−1.39
	LH.7	Model quartzite. B	3	1.04	0.81	1.22	1.02	No	0.81	No	−0.46
	LH.8	Model quartzite. B	4	1.37	1.05	1.32	1.21	No	3.58	No	−2.89
	LH.9	Model quartzite. B	5	1.81	1.17	1.38	1.30	No	4.36	No	0.82
	LH.10	Model quartzite. B	6	2.41	1.58	1.61	1.55	No	5.03	No	0.40
Axisymmetric extension	LH.2	Model quartzite. B	7	0.71	0.17	0.67	0.54	No	4.30	No	−1.70
	LH.3	Model quartzite. B	8	1.04	0.33	0.97	0.71	No	5.77	No	0.72
	LH.4	Model quartzite. B	9	1.31	0.43	1.15	0.88	No	3.37	No	−0.64
	LH.5	Model quartzite. B	10	2.29	0.69	1.68	1.64	No	2.11	No	−0.68
Plane strain	LH.11	Model quartzite. B	11	0.72	0.28	0.77	0.58	No	0.92	No	−4.69
	LH.12	Model quartzite. B	12	0.98	0.43	1.05	0.74	No	1.82	No	2.45
	LH.13	Model quartzite. B	13	1.30	0.61	1.28	0.91	No	0.59	No	−2.4
	LH.14	Model quartzite. B	14	1.70	1.02	1.71	1.21	No	1.58	No	−0.25
	LH.15	Model quartzite. B	15	2.28	0.99	1.66	1.17	No	0.39	No	−11.13
Axisymmetric flattening	Run 5.No.0	Jessell (1988b)	16	0.00	0.02	0.18	0.17	Yes	—	—	—
	Run 5.No.3	Jessell (1988b)	17	0.43	0.13	0.54	0.39	No	3.54	No	5.22
	Run 5.No.7	Jessell (1988b)	18	1.01	0.57	1.02	0.85	No	4.19	No	−4.27
	Run 5.No.15	Jessell (1988b)	19	1.57	0.90	1.27	1.09	No	6.27	No	4.96
	Run 5.No.19	Jessell (1988b)	20	2.66	2.44	2.12	2.04	No	2.21	No	−0.05
Coaxial natural and experimental (see Price 1985)											
Axisymmetric flattening	GB-177	Tullis (1977), exp.	21	1.81	2.03	2.05	1.70	No	2.10	No	4.46
	GB-174	Tullis (1977), exp.	22	1.08	0.78	1.22	0.98	No	9.67	No	8.89
	41504	Dayan (1981)	23	1.01	0.25	0.78	0.55	No	3.47	No	2.05
General flattening	14W-10-16	Compton (1980)	24	0.95	0.44	1.18	0.94	No	5.98	No	3.35
	14W-10-8	Compton (1980)	25	1.06	0.41	1.14	0.95	No	0.44	No	4.13
	14W-14-3	Compton (1980)	26	1.30	0.76	1.88	1.75	No	4.02	No	7.93
	IND-4	Compton (1980)	27	2.07	1.99	4.96	4.09	No	19.99	Yes	13.78
Plane strain	Q66	Mitra & Tullis (1979)	28	0.62	0.16	0.61	0.43	No	3.78	No	2.77
	Q55	Tullis (1977), exp.	29	0.98	0.64	1.35	0.96	No	2.46	No	4.45
	Putney quartzite	Tullis (1977)	30	0.83	0.61	1.26	0.89	No	1.06	No	1.11
	Q41	Tullis (1977)	31	0.98	0.58	1.08	0.84	No	9.52	No	2.00
	41506	Dayan (1981)	32	1.32	0.54	1.38	1.28	No	13.03	Yes	5.65
	Q51	Tullis (1977), exp.	33	1.55	0.48	0.92	0.79	No	5.59	No	5.16
General extension	Weverton quartzite	Tullis (1977)	34	1.09	0.62	1.37	1.00	No	1.29	No	4.60
Axisymmetric extension	Cheshire quartzite	Tullis (1977)	35	0.97	0.60	1.41	1.07	No	6.23	No	4.41
	Antietem quartzite	Tullis (1977)	36	1.41	0.90	1.50	1.07	No	12.13	Yes	7.11
Non-coaxial models (simple shear)											
$\gamma = 0.2$	LH.1	Lister & Hobbs (1980)	37	0.14	0.02	0.20	0.17	Yes	—	—	—
$\gamma = 1.5$	LH.5	Lister & Hobbs (1980)	38	0.98	0.43	1.05	0.74	No	4.85	No	−1.07
$\gamma = 3.0$	LH.7	Lister & Hobbs (1980)	39	1.70	0.87	1.76	1.31	No	23.66	Yes	−9.79
$\gamma = 4.0$	LH.8	Lister & Hobbs (1980	40	2.04	1.17	2.15	1.59	No	26.77	Yes	−12.30
$\gamma = 1.732$	WEN.1	Wenk & Christie (1991)‡ TBH	41	1.11	1.66	2.72	1.99	No	48.76	Yes	11.23
$\gamma = 1.732$	WEN.2	Self-consistent	42	1.11	1.60	2.98	2.28	No	44.50	Yes	11.56
$\gamma = 0.0$	Run 1.No.0	Jessell (1988b)	43	0.00	0.02	0.17	0.12	Yes	—	—	—
$\gamma = 0.57$	Run 1.No.3	Jessell (1988b)	44	0.40	0.14	0.57	0.26	No	1.78	No	−17.76
$\gamma = 1.33$	Run 1.No.7	Jessell (1988b)	45	0.88	0.60	0.98	0.93	No	7.98	No	−7.04
$\gamma = 2.85$	Run 2.No.15	Jessell (1988b)	46	1.63	2.79	3.92	2.81	No	69.41	Yes	13.67
$\gamma = 0.0$	Run 2.No.0	Jessell (1988b)	47	0.00	0.07	0.13	0.10	Yes	—	—	—
$\gamma = 0.57$	Run 2.No.3	Jessell (1988b)	48	0.40	0.09	0.46	0.32	No	7.66	No	−8.68
$\gamma = 1.33$	Run 2.No.7	Jessell (1988b)	49	0.88	1.18	1.97	1.41	No	12.97	No	−7.37
$\gamma = 2.85$	Run 2.No.15	Jessell (1988b)	50	1.63	1.90	3.44	2.62	No	21.98	No	1.25
$\gamma = 0.0$	Run 3.No.0	Jessell (1988b)	51	0.00	0.03	0.26	0.19	Yes	—	—	—
$\gamma = 0.57$	Run 3.No.3	Jessell (1988b)	52	0.40	0.16	0.58	0.44	No	5.46	No	−7.84
$\gamma = 1.33$	Run 3.No.7	Jessell (1988b)	53	0.88	0.68	1.06	0.96	No	18.56	Yes	4.92
$\gamma = 2.85$	Run 3.No.15	Jessell (1988b)	54	1.63	3.26	4.42	3.14	No	73.33	Yes	16.54
$\gamma = 0.0$	Run 4.No.0	Jessell (1988b)	55	0.00	0.07	0.42	0.34	Yes	—	—	—
$\gamma = 1.71$	Run 4.No.9	Jessell (1988b)	56	1.10	0.58	1.14	0.84	No	0.63	No	−6.60
$\gamma = 3.61$	Run 4.No.19	Jessell (1988b)	57	1.91	2.25	3.20	2.29	No	45.28	Yes	5.80
$\gamma = 5.51$	Run 4.No.29	Jessell (1988b)	58	2.46	3.09	5.06	3.73	No	66.49	Yes	6.18
$\gamma = 5.0$	JL.a	Jessell & Lister (1990)‡	59	2.33	1.09	2.31	1.84	No	58.97	Yes	9.13
$\gamma = 5.0$	JL.b	Jessell & Lister (1990)‡	60	2.33	1.54	2.97	2.30	No	70.44	Yes	10.34
$\gamma = 5.0$	JL.c	Jessell & Lister (1990)‡	61	2.33	0.83	1.95	1.65	No	40.96	No	11.30
$\gamma = 5.0$	JL.d	Jessell & Lister (1990)‡	62	2.33	0.62	1.45	1.11	No	20.97	No	16.39
$\gamma = 5.0$	JL.e	Jessell & Lister (1990)‡	63	2.33	3.94	4.32	3.14	No	12.14	No	8.16
Non-coaxial natural and experimental											
General shear	1	Mancktelow (1987)	64	—	0.84	2.07	2.00	No	24.00	Yes	11.91
	2	Mancktelow (1987)	65	—	1.11	2.93	2.66	No	30.32	Yes	14.70
	3	Mancktelow (1987)	66	—	1.14	2.81	2.44	No	28.27	Yes	9.90
General shear	SG.1	Law (1987)	67	—	0.79	1.92	1.73	No	24.22	Yes	16.44
	SG.2.1.	Law (1987)	68	—	0.55	1.39	1.36	No	14.21	Yes	6.87
	SG.2.2	Law (1987)	69	—	0.50	1.32	1.13	No	17.07	Yes	13.18
	SG.2.3	Law (1987)	70	—	0.62	1.52	1.24	No	23.49	Yes	12.11
	SG.2.4	Law (1987)	71	—	0.64	1.57	1.31	No	21.80	Yes	12.96
	SG.2.5	Law (1987)	72	—	0.49	1.28	1.02	No	16.57	Yes	8.69
	SG.3	Law (1987)	73	—	0.64	1.60	1.50	No	5.20	No	0.86
	SG4.	Law (1987)	74	—	0.58	1.46	1.23	No	8.16	No	2.1
Experimental, simple shear (ice)	BD.1	Bouchez & Duval in: Etchecopar & Vasseur (1987)‡	75	0.42	1.27	1.93	1.36	No	9.52	No	8.72
	BD.2		76	0.65	1.04	1.50	1.43	No	9.32	No	2.19
	BD.3		77	1.25	2.32	2.43	1.84	No	48.27	Yes	21.56

*This field refers to the number assigned to the fabrics in this work.

†Dextral obliquity: positive; sinistral obliquity: negative.

‡The following fabrics are not specifically labelled by the authors. Lister & Hobbs (1980, fig. 8), their fabrics are here numbered from the less to the more deformed ones, within a given strain field. Wenk & Christie (1991, fig. 9). Jessell & Lister (1990, fig. 3); from *low* to *high* temperatures. Bouchez & Duval in Etchecopar & Vasseur (1987, fig. 7b).

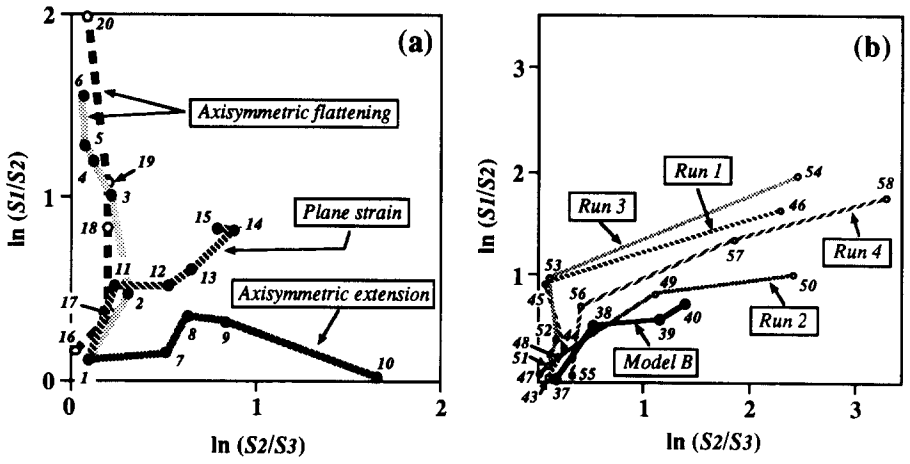

Fig. 4. Modelled fabrics plotted in Woodcock diagrams. The numbers indicated are those listed in Table 1. (a) Coaxial models. Lister & Hobbs (1980), black circles; Jessell (1988b), open circles (Run 5). (b) Non-coaxial models. Lister & Hobbs (1980), black circles (Model B); Jessell (1988b), small open circles (Runs 1–4).

of Wenk & Christie (1991) that the fabrics with maxima representing a dynamic state (developed in simple shear as an example) never become very intense: it is important to realize that the disappearance of a leg in a crossed-girdle pattern can induce a marked increase in the strength of a fabric, especially when factors based on eigenvalue computation are used. In fact the higher fabric intensities occur when external asymmetry is reached (Table 1).

Asymmetry and obliquity

For coaxial deformations the *Am* parameter is constant when the deformation intensity (*D*) increases (Table 1). In non-coaxial deformations *Am* evolves in a very different way: the first shearing stages produce symmetric fabrics that become asymmetric when γ (shear strain) increases above a certain value (Schmid & Casey 1986).The critical shear strain is a prime function of the model considered, and seems to be larger when the model attempts to simulate higher temperature deformation (Run 2 of Jessell 1988b, or fabrics 'd' and 'e' in fig. 3 of Jessell & Lister 1990). An explanation for this may be that high temperatures induce a strong accumulation of poles near the *Y*-axis, so that the distribution of δs moves towards $\pm$ 90°. An increase in symmetry follows. The linear histograms show different patterns when fabrics resulting from coaxial or non-coaxial deformations are considered. In the first case two symmetric maxima are defined (Fig. 5a), while in the second, one maximum comes to dominate over the other (Fig. 5b), which eventually vanishes when *D* is high enough (cf. Bouchez & Pécher 1976, Etchecopar 1977). Several models of non-coaxial *c*-axis fabric development here are analysed. They correspond to simple-shear deformation and are essentially based on the TBH theory (Lister & Hobbs 1980, model B), although more comprehensive models based on the combination of lattice rotations following the TBH theory and recrystallization processes are also considered (Jessell 1988a,b, Jessell & Lister 1990). Finally the viscoplastic approach of Wenk *et al.* (1989) and Wenk & Christie (1990) was checked as well. Relative values of critical resolved shear stress (CRSS) for the main slip systems in quartz, grain boundary mobilities and recovery rates are the main input parameters in the TBH models. The possibility that different models could lead to contrasted δ distributions or perhaps to opposite α_f values for the same bulk shear sense is a central point in this work. When natural and experimental non-coaxial fabrics are analysed (Table 1, numbers 64–77) *Am* is often large and α_f is positive for dextral shear, although the fabrics are not necessarily a consequence of simple-shearing histories, and may involve besides a component of coaxial flow (e.g. Law 1987). In the models by Lister & Hobbs (1980) where recrystallization processes are not considered, distinct fabrics are obtained depending on the CRSS values: Models A and B with a predominant basal ⟨*a*⟩ slip system develop very similar linear intensity distributions (cf. rose-diagrams in figs. 12 and 13 of Lister & Hobbs 1980). A maximum of intensity in the quadrant pair opposite to the imposed shear sense results, and consequently α_f has negative values for asymmetric fabrics under dextral shearing (Table 1, fabrics 39 and 40; here only Model B was studied). The same discrepancy was shown by Bouchez *et al.* (1983), but see also Simpson (1980), García Celma (1982), Simpson & Schmid (1983) and Mancktelow (1987) for additional discussions. Model C of Lister & Hobbs (1980) with simultaneous predominant activity of basal ⟨*a*⟩ and prism ⟨*a*⟩ slip systems exhibit more evenly populated quadrants (cf. Lister & Hobbs 1980, Fig. 14). In contrast, models which combine the predictions of the TBH theory with recrystallization (Jessell 1988b, Jessell & Lister 1990) invariably produce positive obliquity for asymmetric fabrics (Fig. 5b and Table 1). This is so with independence of the active slip systems, work hardening rate or dynamic recovery rate. Similar results are obtained for the viscoplastic TBH or viscoplastic self-consistent models (numbers 41 and 42 in Table 1). Note, however, in Table 1 that α_f attains negative values during the first deformational stages when the fabrics are still symmetrical. This could be interpreted as a consequence of the *c*-axis kinematics in the early stages of fabric development (see e.g. Jessell

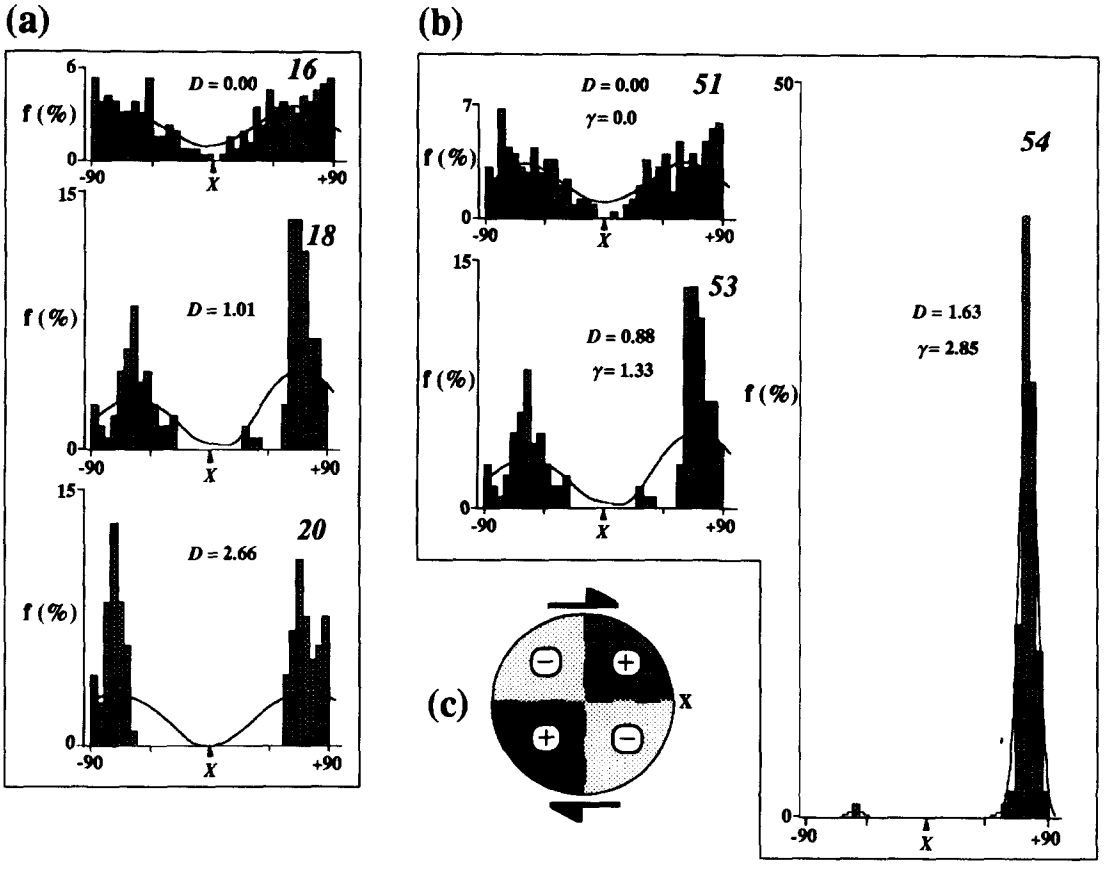

Fig. 5. Linear histograms of δ values for different selected model sequences. Interval of classes: 5°. A smoothing curve is added to each histogram. (a) Axisymmetric flattening, Run 5 of Jessell (1988b). (b) Simple shear, Run 3 of Jessell (1988b). (c) Shear sense for non-coaxial deformation, and δ sign criterion in terms of the quadrant division. D represents the value of the finite strain intensity. Numbers in italics refer to the fabric numbers in Table 1. The distribution is statistically isotropic (random) in fabrics 16 and 51.

1988a, Wenk *et al.* 1989). The coincidence with natural and experimental fabrics tend to support the intensity distributions attained by models with coupled lattice rotations and dynamic recrystallization, such as that of Jessell (1988b) and Jessell & Lister (1990), in which α_f is positive for dextral shear (Fig. 5b). Following the procedure outlined in the previous section, the α_f angle for the fabrics with proven external asymmetry appears to be a reliable kinematic criterion.

When we plot the obliquity angle with respect to D, we find that the variation is small and oscillatory (between ± 5°) for coaxial deformations, α_f decreasing towards 0° when the deformation increases (Fig. 6a). In non-coaxial paths the obliquity exceeds significantly the

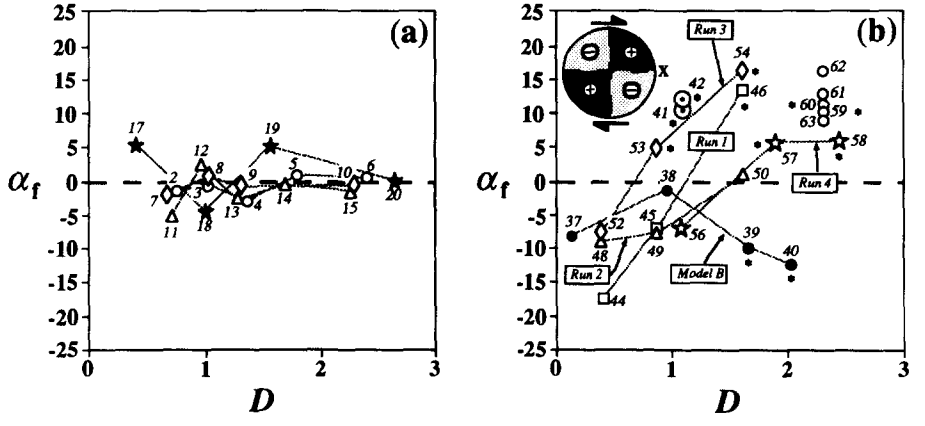

Fig. 6. α_f evolution with deformation. (a) Coaxial models. Lister & Hobbs (1980): open circles (axisymmetric flattening); triangles (plane strain); rhombs (axisymmetric extension). Jessell (1988b): filled stars (Run 5). (b) Non-coaxial models. Lister & Hobbs (1980): Model B. Jessell (1988b): Runs 1–4. Jessell & Lister (1990): open circles. Wenk & Christie (1991): centered circles. The inset shows the shear sense in non-coaxial deformations. Asterisks indicate the asymmetric fabrics according to the *Am* test. See Fig. 3 for the α_f sign criterion.

Table 2. Results of the empirical fitting of the critical external asymmetry factor in terms of n (number of poles). The general fitting equation has the form:

$$|Am_c| = a \cdot n^b;\ n > 200;\ Am \text{ in absolute value}$$

Level of significance (α)	a	b	Correlation coefficient
0.1	103.98	−0.484	0.90
0.05	130.72	−0.494	0.90
0.01	171.38	−0.494	0.90

± 5° limit (Fig. 6b) and once the external asymmetry is achieved α_f is high, and its sign agrees with the imposed shear sense in the manner already discussed (except for the samples 37–40). Inspection of Fig. 6(b) suggests that for basal ⟨a⟩ slip controlling the fabric development and for a given D value, high recrystallization rates (Runs 1 and 3) promote larger positive obliquities and asymmetries than those obtained when the grain boundary mobility is restricted (Run 4). As shown before, the Am test reveals symmetry in models simulating higher temperatures (larger activity of the prism ⟨a⟩ slip system) even if considerable recrystallization rates are introduced (Run 2). Lower α_f values are also developed for higher temperatures assuming the same recrystallization activity (compare Runs 1 and 2).

A graphical way of determining external symmetry in quartzites: the Am/n graph

Equation (4) was applied to all the samples in Table 1, and the Am_c critical values were computed and plotted in terms of the number of poles (n). Three different levels of significance were considered (Figs. 7a–c). For $n > 200$ the plots show a good fit with the curve defined by equation (4) (Table 2). No significant differences can be measured between fabrics generated by natural, experimental or theoretical processes and they are not distinguished in Fig. 7. The a coefficient in Table 2 is a direct function of S_{Am} and indicates a remarkable homogeneity between fabrics in the standard deviation of δ values for a given level of significance. Note in Table 2 the proximity of the b coefficient to its theoretical value in equation (4): − 0.5. The acceptable fit between the empirical data and the equation (4) seems to be good support for the analytical assumptions followed in the method. In Fig. 7(d) the three critical curves are represented in a single Am/n graph; these curves allow direct estimation of the asymmetry of fabrics in quartzites. The pattern with vertical lines in Fig. 7(d) indicates the field of external symmetric fabrics for a significance level (α) equal to 0.1. Similarly the fields below the 0.05 and 0.01 curves are the regions of external symmetry for significance levels equal to 0.05 and 0.01, respectively. The area above the curves is the region of asymmetry for each specific level of significance, so the region with light gray pattern marks the rejection field for $\alpha = 0.01$. When $n < 200$ the value of the correlation coefficient is considerably reduced, so this is the critical minimum number of poles to be measured in order to apply the

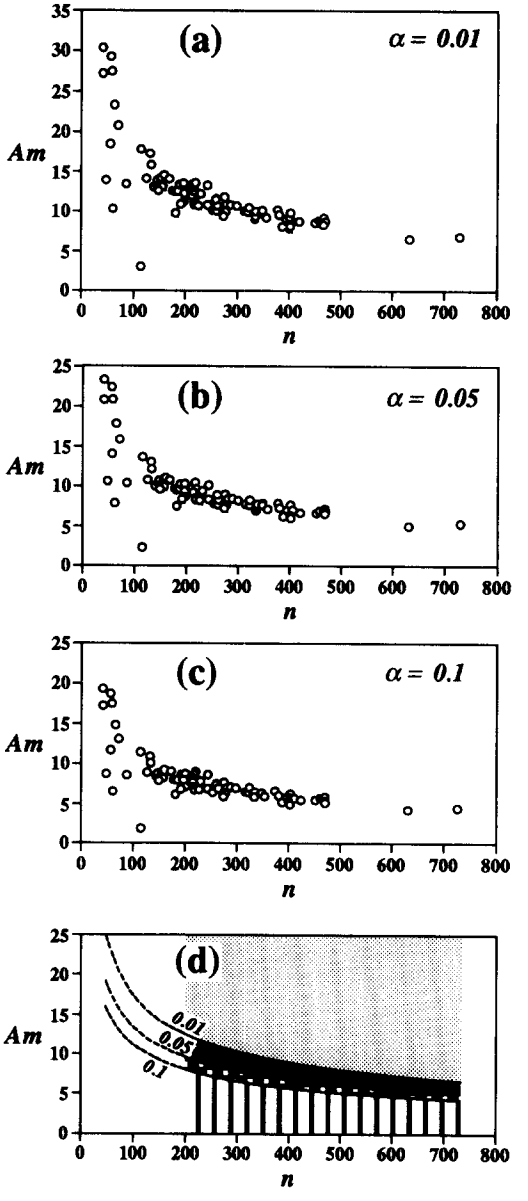

Fig. 7. Critical values of the asymmetry factor, Am, for all the studied fabrics. (a) Significance level (α): 0.01. (b) $\alpha = 0.05$. (c) $\alpha = 0.1$. (d) Curves of Am critical values obtained from (a), (b) and (c) and for $n > 200$ (see Table 2). Areas with $n < 200$ are marked with discontinuous curves. See text for explanation.

method, at least from a statistical perspective. The area of discontinuous lines in Fig. 7(d) corresponds exactly to the $n < 200$ condition. This recommended minimum number of points must represent an equivalent number of different original grains, as in the models here analysed, where the initial orientation population is always isotropic (Table 1). In a recent paper Lloyd *et al.* (1992) discuss the crystal fabric evolution in a quartzofeldspathic mylonitic shear zone from Torridon (Scotland), showing how a large number of recrystallized grains could represent only a few dozen parent grains. In this case the prerequisite of initial isotropic fabric is seldom fulfilled, and an erroneous shear sense may be deduced from Am and α_f when 200 recrystallized grains are measured in a limited area corresponding perhaps to the one individual original grain. Meso- and microstructural observations are essential to ascertain whether the

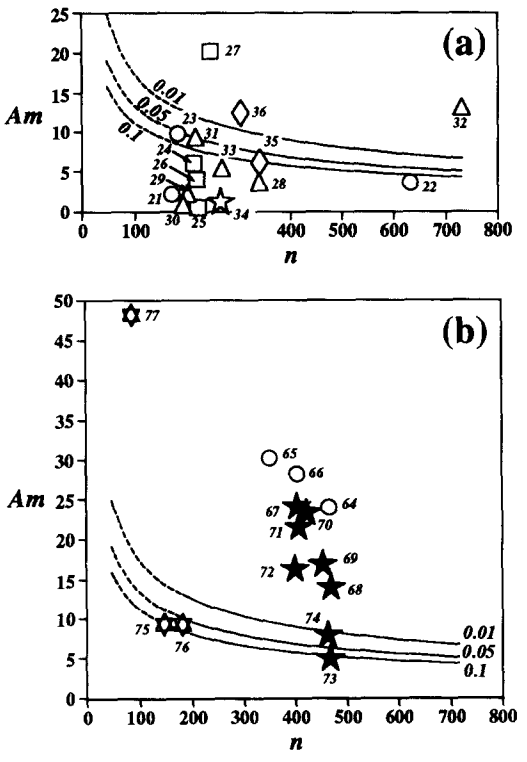

Fig. 8. *Am/n* diagrams of natural and experimental quartz *c*-axis fabrics. (a) Coaxial examples. (b) Non-coaxial examples. See sample sources in Table 1.

original constraints of a given method of fabric analysis are violated, and the method needs to be applied with care.

The *Am* values of natural and experimental fabrics in Table 1 are plotted against *n* (Fig. 8). Coaxial fabrics displays small *Am* values (Fig. 8a), however the samples 27 (IND-4, Compton 1980), 32 (41506, Dayan 1981) and 36 (Antietem quartzite, Tullis 1977) show external asymmetry, and possibly point to a non-coaxial history (see Price 1985, p. 399, for a discussion of IND-4). In contrast non-coaxial fabrics fall well within the asymmetric field (Fig. 8b). Only four samples could be considered as symmetric for a very exigent level of significance ($\alpha = 0.01$): samples 73 and 74 (SG.3 and SG.4 of Law 1987) correspond to a sub-simple shearing deformation (De Paor 1983), with a dominant coaxial component. Samples 75 and 76 represent the first stages of an experimental simple shearing history in ice, with $\gamma < 1$.

The significance of the critical curves is essentially empirical, as the values of the *a* and *b* coefficients in Table 2 were obtained from a number of real or computed fabrics. However, the nature of the pole figures analysed (well-defined diagrams with known deformational histories) and the identical results achieved from the diverse sources (natural, experimental and theoretical) give confidence in the use of the *Am/n* graph.

DISCUSSION AND CONCLUSIONS

Theoretical, experimental and natural quartz *c*-axis fabrics that develop during a single event of intense deformation, and in monomineralic aggregates, usually display a well-defined skeletal outline. The skeleton can be modified during the last episodes of a long and complex deformation history, while the distribution intensity does not apparently alter to the same degree (Lister & Williams 1979, Behrmann & Platt 1982, Passchier 1983). The presence of additional mineral phases often makes fabric interpretation difficult (Starkey & Cutforth 1978, White *et al.* 1980, Miller & Christie 1981, Passchier 1983, Lisle 1985). In addition the study of CPOs originating during heterogeneous deformation is by no means easy (e.g. García Celma 1982, Law 1987), and it is necessary to make a large number of fabric determinations (Bouchez *et al.* 1983).

The method described here aims to decipher a variety of aspects of complex fabrics, such as their asymmetrical nature with respect to an external reference frame. Nevertheless some restrictions must be taken into account when attempting to compute the *Am* and α_f parameters in a *c*-axis sub-fabric.

(1) A quartz *c*-axis pole figure is only a sub-fabric of the whole crystallographic orientation. Therefore the symmetry of the whole CPO is not proven through the mere determination of the symmetry of a single sub-fabric. Fortunately asymmetric *c*-axis fabrics imply asymmetric CPOs and therefore non-coaxial flow patterns, provided original isotropy and a steady deformation history.

(2) This method is a linear bidimensional approach. As a consequence information is lost concerning the particular position of maxima and only statistically significant differences between quadrants in the projection can be analysed. Very irregular triclinic fabrics may give misleading estimations when analysed on these grounds.

(3) The external reference frame must be well established because a shift in the position of the *X*-axis (zero direction) can greatly affect the *Am* estimation.

(4) The statistical obliquity (α_f) can be read as a shear sense indicator when models based on the combination of TBH theory and recrystallization processes, or viscoplastic behaviours, are considered. Compatibility with natural fabrics is good, in spite of deviation from simple-shearing flow that seems to be common in natural shear zones. In contrast models considering only the TBH theory may exhibit opposite obliquity angles. Clearly more data are needed from new theoretical models approaching sub-simple shearing and accounting for a larger variety of intrinsic factors (Hobbs 1985) before a more general validity can be attributed to *Am* and α_f.

(5) To obtain reliable results it is advisable to measure at least 200 poles per sample. Meso- and microstructural criteria must be used to help decide the optimum sampling scheme, which can be very variable depending on the specific geological situation.

The *Am* and α_f computations in several published *c*-axis pole figures seem to reflect the observed fabric evolution accurately. The combination of both parameters constitutes a reliable new kinematic criterion under the conditions discussed before. Critical values of

Am can be represented graphically and constitute a rapid way to the evaluation of asymmetry in quartzites.

The method has been also applied by Fernández-Rodríguez (1991) to check the statistical symmetry of more than 200 quartz *c*-axis fabric diagrams belonging to a regional shear zone. As distinct from theoretical models, deformation history is sub-simple shearing and rocks are inhomogeneous polymineralic aggregates, mostly gneissic. Accordingly the pole figures are more vague than in the fabrics here analysed and the skeleton outline is seldom sharp. Seventy per cent of fabrics with external asymmetry showed an obliquity angle compatible with the bulk movement in the shear zone. This percentage agrees with the results in other studies (Passchier 1983, Law *et al.* 1984). The 30% of asymmetric fabrics with contrary α_f are believed to be a consequence of the inhomogeneous flow pattern as they are more represented in the boundaries of the shear zone, where coaxial flow predominates and meso- and microstructural indicators are inconclusive or even opposite. In this case the Am/α_f method could provide some insight in deciphering vague quartz *c*-axis fabrics from gneissic rocks. Nevertheless, as indicated before, more comprehensive models are needed, specially to simulate heterogeneous sub-simple flow in complex polymineralic aggregates.

A quantitative comparison among fabrics can also be attempted. For instance, the highest increase in *Am* with respect to *D* is found in the Runs 1 and 3 of Jessell (1988b) (Table 1); meanwhile in Run 2 or in the high-temperature simulations of Jessell & Lister (1990), *Am* does not reach the critical value for symmetry rejection. These observations are consistent with those of García Celma (1982) and Schmid & Casey (1986) in the sense that the quartz *c*-axis fabrics with a single maximum close to the *Y* axis do not give a good kinematic criterion.

In order to compare the asymmetry parameters based on the definition of the skeletal outline with *Am* and α_f we have investigated eight *c*-axis fabrics measured by Law (1987) in his study of the Moine Thrust at the Stack of Glencoul (Assynt mylonites). Two external asymmetry factors are used by Law: first the obliquity of the 'central girdle segment with respect to the foliation trace' (Law 1987, angle ψ); second the angles c_1 and c_2 between the *Z* strain axis and the leading and trailing peripheral legs of the fabric skeleton, respectively. We computed also the *Am* and α_f parameters of these fabrics. As Law has shown, the asymmetry increases towards the thrust plane (Table 1 and Fig. 9a). The change in ψ with respect to *Am* or α_f has the following significance (Figs. 9b & c): the path from SG.3, statistically symmetric, to SG.4, slightly asymmetric, involves a decrease in ψ, that is to say, an increase in the skeleton asymmetry (Fig. 9d, left and central sketches). A minimum value of ψ is reached (sample SG.2.1), and afterwards ψ shows a direct correlation with *Am* or α_f, i.e. the central girdle segment has a tendency to be reoriented normal to the *XY* plane of the finite strain ellipsoid when the statistic asymmetry (*Am* and α_f) becomes more and more intense, or, in other words, the skeleton symmetry

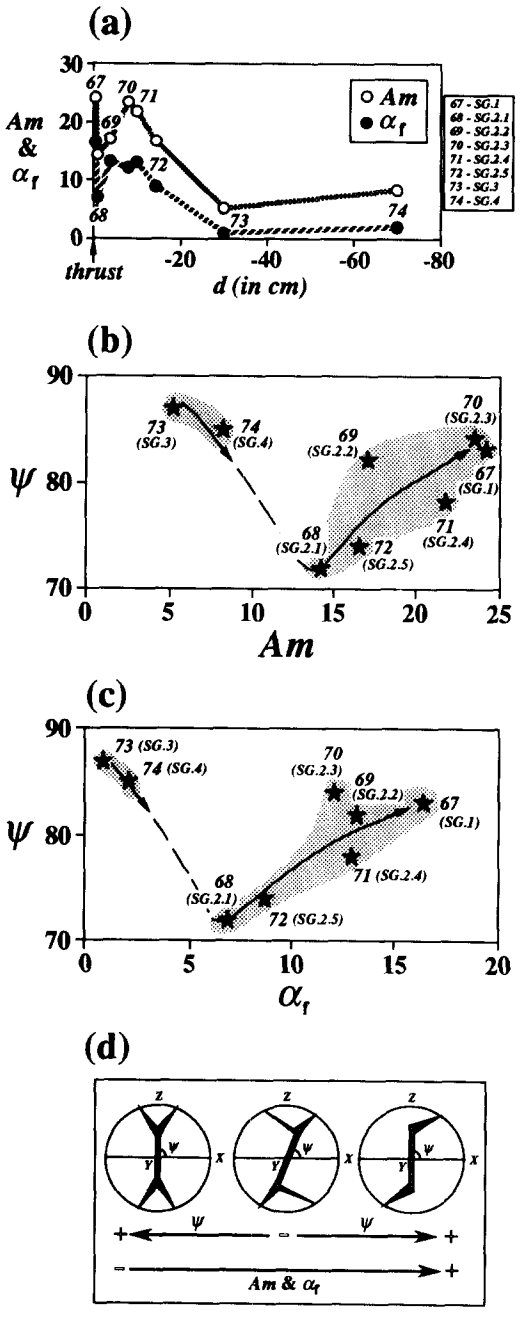

Fig. 9. (a) Variation of *Am* and α_f beneath the Moine Thrust at the Stack of Glencoul (Scotland). Samples measured by Law (1987). Inset: equivalence between the fabric numbers in Table 1 and the Law's labels. (b) & (c) Relationships between the angle ψ describing the external asymmetry of the fabric skeleton (Law 1987) and the *Am* and α_f factors for the same samples. (d) Schematic representation of the evolution of these fabrics in terms of the skeleton-based (ψ) and distribution intensity-based (*Am* and α_f) parameters. See text for further details and discussion.

defined by ψ is larger in the more asymmetric fabrics than in the ones representing the first stages of statistical asymmetry (Fig. 9d, right and central sketches, respectively). This is a somewhat surprising result, whose explanation is well beyond the limits of this work. The results agree with Law's statement that "SG.1 and SG.2 are strongly asymmetrical with respect to foliation and lineation, both in terms of intensity distribution and, to a lesser extent, skeletal outline". It seems that, in fact, the *Am* and α_f parameters are quite sensitive to progressive

tendencies towards asymmetry present in some natural rocks. Therefore, when the evaluation of the external asymmetry degree of quartz *c*-axis fabrics in a shear zone is attempted, the measure of skeleton-based angles can be satisfactorily completed with the computation of the Am and α_f parameters.

In conclusion the method outlined in this work is thought to describe numerically a variety of aspects of the external asymmetry and obliquity of quartz *c*-axis fabric diagrams. The simplicity of the method, and its numerical character can be useful in the study of single fabrics and in the comparison of a large number of complex fabrics coming from different sources.

Acknowledgements—Comments by Professor S. H. White aided considerably in previous versions of this work. Special thanks are due to Professor R. Capote, Dr A. Castro, Dr I. Moreno-Ventas, Dr R. Bateman and M. V. Perelló for constructive suggestions and assistance. We thank Mark Jessell and an anonymous reviewer for their helpful critical reviews. This paper has greatly benefited from comments and editorial advice of C. W. Passchier. The English text has been greatly improved by Dr R. Bateman. Financial support was provided by the Universidad Complutense de Madrid (project 2490); a Spanish M.E.C. studentship grant is gratefully acknowledged by C. Fernández-Rodríguez.

REFERENCES

Behrmann, J. H. & Platt, J. P. 1982. Sense of nappe emplacement from quartz *c*-axis fabrics: an example from the Betic Cordilleras (Spain). *Earth Planet. Sci. Lett.* **59**, 208–215.

Bouchez, J.-L. 1977. Plastic deformation of quartzites at low temperature in an area of natural strain gradient. *Tectonophysics* **39**, 25–50.

Bouchez, J.-L., Lister, G. S. & Nicolas, A. 1983. Fabric asymmetry and shear sense in movement zones. *Geol. Rdsch.* **72**, 401–419.

Bouchez, J.-L. & Pécher, A. 1976. Plasticité du quartz et sens de cisaillement dans les quartzites du grand chévauchement himalayen. *Bull. Soc. géol. Fr., Sér.* 7 **18**, 1377–1385.

Bouchez, J.-L. & Pécher, A. 1981. The Himalayan Main Central Thrust pile and its quartz-rich tectonites in Central Nepal. *Tectonophysics* **78**, 23–50.

Brunel, M. 1980. Quartz fabrics in shear-zone mylonites: evidence for a major imprint due to late strain increments. *Tectonophysics* **64**, T33–T44.

Bunge, H. J. 1969. *Mathematische Methoden der Texturanalyse*. Akademie, Berlin.

Bunge, H. J. 1985. Representation of preferred orientations. In: *Preferred Orientation in Deformed Metals and Rocks: An Introduction to Modern Texture Analysis* (edited by Wenk, H.-R.). Academic Press, Orlando, 73–108.

Compton, R. R. 1980. Fabrics and strains in quartzites of a metamorphic core complex, Raft River Mountains, Utah. In: *Cordilleran Metamorphic Core Complexes* (edited by Crittenden, M. D., Coney, P. J. & Davis, G. H.). *Mem. geol. Soc. Am.* **153**, 385–398.

Davis, J. C. 1986. *Statistics and Data Analysis in Geology*. John Wiley & Sons, New York.

Dayan, H. 1981. Deformation studies of the folded mylonites of the Moine Thrust, Eriboll, Northwest Scotland. Unpublished Ph.D. thesis, University of Leeds.

Dell'Angelo, L. N. & Tullis, J. 1986. A comparison of quartz *c*-axis preferred orientations in experimentally deformed aplites and quartzites. *J. Struct. Geol.* **8**, 683–692.

Dell'Angelo, L. N. & Tullis, J. 1989. Fabric development in experimentally sheared quartzites. *Tectonophysics* **169**, 1–21.

De Paor, D. G. 1983. Orthographic analysis of geological structures—I. Deformation theory. *J. Struct. Geol.* **5**, 255–277.

Etchecopar, A. 1977. A plane kinematic model of progressive deformation in a polycrystalline aggregate. *Tectonophysics* **39**, 121–139.

Etchecopar, A. & Vasseur, G. 1987. A 3-D kinematic model of fabric development in polycrystalline aggregates: comparisons with experimental and natural examples. *J. Struct. Geol.* **9**, 705–717.

Fernández-Rodríguez, C. 1991. Estudio de los procesos de deformación en la Zona de Cizalla de Hiendelaencina (Sistema Central Español). Unpublished PH.D. thesis, Universidad Complutense de Madrid.

Fisher, N. I., Lewis, T. & Embleton, B. J. J. 1987. *Statistical Analysis of Spherical Data*. Cambridge University Press, Cambridge.

García Celma, A. 1982. Domainal and fabric hererogeneities in the Cap de Creus quartz mylonites. *J. Struct. Geol.* **4**, 443–455.

Hobbs, B. E. 1985. The geological significance of microfabric analysis. In: *Preferred Orientation in Deformed Metals and Rocks: An Introduction to Modern Texture Analysis* (edited by Wenk, H.-R.). Academic Press, Orlando, 463–484.

Jessell, M. W. 1988a. Simulation of fabric development in recrystallizing aggregates—I. Description of the model. *J. Struct. Geol.* **10**, 771–778.

Jessell, M. W. 1988b. Simulation of fabric development in recrystallizing aggregates—II. Example model runs. *J. Struct. Geol.* **10**, 779–793.

Jessell, M. W. & Lister, G. S. 1990. A simulation of the temperature dependence of quartz fabrics. In: *Deformation Mechanisms, Rheology and Tectonics* (edited by Knipe, R. J. & Rutter, E. H.). *Spec. Publs geol. Soc. Lond.* **54**, 353–362.

Laurent, Ph. & Etchecopar, A. 1976. Mise en évidence à l'aide de la fabrique du quartz d'un cisaillement simple à déversement ouest dans le Massif de Dora Moire (Alpes Occidentales). *Bull. Soc. géol. Fr., Sér.* 7, **18**, 1387–1393.

Law, R. D. 1987. Heterogeneous deformation and quartz crystallographic fabric transitions: natural examples from the Stack of Glencoul, northern Assynt. *J. Struct. Geol.* **9**, 819–833.

Law, R. D. 1990. Crystallographic fabrics: a selective review of their applications to research in structural geology. In: *Deformation Mechanisms, Rheology and Tectonics* (edited by Knipe, R. J. & Rutter, E. H.). *Spec. Publs geol. Soc. Lond.* **54**, 335–352.

Law, R. D., Knipe, R. J. & Dayan, H. 1984. Strain path partitioning within thrust sheets: microstructural and petrofabric evidence from the Moine Thrust Zone at Loch Eriboll, Northwest Scotland. *J. Struct. Geol.* **6**, 477–497.

Lisle, R. J. 1985. The use of the orientation tensor for the description and statistical testing of fabrics. *J. Struct. Geol.* **7**, 15–117.

Lister, G. S. 1977. Discussion: Crossed girdle *c*-axis fabrics in quartzites plastically deformed by plane strain and progressive simple shear. *Tectonophysics* **39**, 51–54.

Lister, G. S. & Hobbs, B.E, 1980. The simulation of fabric development during plastic deformation and its application to quartzite: the influence of deformation history. *J. Struct. Geol.* **2**, 355–370.

Lister, G. S. & Paterson, M. S. 1979. The simulation of fabric development during plastic deformation and its application to quartzite: fabric transitions. *J. Struct. Geol.* **1**, 99–115.

Lister, G. S., Pateson, M. S. & Hobbs, B. E. 1978. The simulation of fabric development during plastic deformation and its application to quartzite: The model. *Tectonophysics* **45**, 107–158.

Lister, G. S. & Price, G. P. 1978. Fabric development in a quartz–feldespar mylonite. *Tectonophysics* **49**, 37–78.

Lister, G. S. & Williams, P. F. 1979. Fabric development in shear zones: theoretical controls and observed phenomena. *J. Struct. Geol.* **1**, 283–297.

Lloyd, G. E., Law, R. D., Mainprice, D. & Wheeler, J. 1992. Microstructural and crystal fabric evolution during shear zone formation. *J. Struct. Geol.* **14**, 1079–1100.

Mancktelow, N. S. 1987. Quartz textures from the Simplon Fault Zone, southwest Switzerland and north Italy. *Tectonophysics* **135**, 133–153.

Mardia, K. V. 1972. *Statistics of Directional Data*. Academic Press, London.

Miller, D. M. & Christie, J. M. 1981. Comparison of quartz microfabric with strain in recrystallized quartzite. *J. Struct. Geol.* **3**, 129–141.

Mitra, S. & Tullis, J. 1979. A comparison of intracrystalline deformation in naturally and experimentally deformed quartzites. *Tectonophysics* **53**, T21–T27.

Passchier, C. W. 1983. The reliability of asymmetric *c*-axis fabrics of quartz to determine sense of vorticity. *Tectonophysics* **99**, T9–T18.

Paterson, M. S. & Weiss, L. E. 1961. Symmetry concepts in the structural analysis of deformed rocks. *Bull. geol. Soc. Am.* **72**, 841–882.

Platt, J. P. & Behrmann, J. H. 1986. Structures and fabrics in a crustal scale shear zone, Betic Cordilleras, SE Spain. *J. Struct. Geol.* **8**, 15–34.

Price, G. P. 1985. Preferred orientations in quartzites. In: *Preferred Orientations in Deformed Metals and Rocks: An Introduction to Modern Texture Analysis* (edited by Wenk, H.-R.). Academic Press, Orlando, 385–406.

Ralser, S. 1990. Shear zones developed in an experimentally deformed quartz mylonite. *J. Struct. Geol.* **12**, 1033–1045.

Ralser, S., Hobbs, B. E. & Ord. A. 1991. Experimental deformation of a quartz mylonite. *J. Struct. Geol.* **13**, 837–850.

Ramsay, J. G. & Huber, M. I. 1983. *The Techniques of Modern Structural Geology, Volume* 1: *Strain Analysis*. Academic Press, London.

Scheidegger, A. E. 1965. On the statistics of the orientation of bedding planes, grain axes and similar sedimentological data. *Prof. Pap. U.S. geol. Surv.* **525C**, 164–167.

Schmid, S. M. & Casey, M. 1986. Complete fabric analysis of some commonly observed quartz c-axis patterns. In: *Mineral and Rock Deformation: Laboratory Studies—The Paterson Volume* (edited by Hobbs, B. E. & Heard, M. C.). *Am. Geophys. Un. Geophys. Monogr.* **36**, 263–286.

Schmid, S. M., Casey, M. & Starkey, J. 1981. An illustration of the advantages of a complete texture analysis described by the orientation distribution function (ODF) using quartz pole figure data. *Tectonophysics* **78**, 101–117.

Schmidt, W. 1925. Gefügestatistik Tschermaks. *Miner. Petrogr. Mitt.* **38**, 392–423.

Simpson, C. 1980. Oblique girdle orientation patterns of quartz *c*-axis patterns from a shear zone in the basement core of the Maggia Nappe, Ticino, Switzerland. *J. Struct. Geol.* **2**, 243–247.

Simpson, C. & De Paor, D. G. 1993. Strain and kinematic analysis in general shear zones. *J. Struct. Geol.* **15**, 1–20.

Simpson, C. & Schmid, S. M. 1983. An evaluation of criteria to deduce the sense of movement in sheared rocks. *Bull. geol. Soc. Am.* **94**, 1281–1288.

Starkey, J. & Cutforth, C. 1978. A demonstration of the interdependence of the degree of quartz preferred orientation and the quartz content of deformed rocks. *Can. J. Earth Sci.* **15**, 841–847.

Tullis, J. 1977. Preferred orientation of quartz produced by slip during plane strain. *Tectonophysics* **39**, 87–102.

Tullis, J., Christie, J. M. & Griggs, D. T. 1973. Microstructures and preferred orientations of experimentally deformed quartzites. *Bull. geol. Soc. Am.* **84**, 297–314.

Turner, F. J. & Weiss, L. E. 1963. *Structural Analysis of Metamorphic Tectonites*. McGraw-Hill, New York.

Weiss, L. E. & Wenk, H.-R. 1985. Symmetry of pole figures and textures. In: *Preferred Orientation in Deformed Metals and Rocks: An Introduction to Modern Texture Analysis* (edited by Wenk, H.-R.). Academic Press, Orlando, 49–72.

Wenk, H.-R., Canova, G., Molinari, A. & Kocks, V. F. 1989. Viscoplastic modeling of texture development in quartzite. *J. geophys. Res.* **94B**, 17,895–17,906.

Wenk, H.-R. & Christie, J. M. 1991. Comments on the interpretation of deformation textures in rocks. *J. Struct. Geol.* **13**, 1091–1110.

White, S. H., Burrow, S. E., Carreras, J. & Shaw, N. D. 1980. On mylonites in ductile shear zones. *J. Struct. Geol.* **2**, 175–187.

Woodcock, N. H. 1977. Specification of fabric shapes using an eigenvalue method. *Bull. geol. Soc. Am.* **88**, 1231–1236.

Woodcock, N. H. & Naylor. M. A. 1983. Randomness testing in three-dimensional orientation data. *J. Struct. Geol.* **5**, 539–548.